REPORT DOCUMENTATION PAGE

Form Approved
OMB No. 0704-0188

Public reporting burden for this collection of information is estimated to average 1 hour per response, including the time for reviewing instructions, searching existing data sources, gathering and maintaining the data needed, and completing and reviewing the collection of information. Send comments regarding this burden estimate or any other aspect of this collection of information, including suggestions for reducing this burden, to Washington Headquarters Services, Directorate for Information Operations and Reports, 1215 Jefferson Davis Highway, Suite 1204, Arlington, VA 22202-4302, and to the Office of Management and Budget, Paperwork Reduction Project (0704-0188), Washington, DC 20503.

1. AGENCY USE ONLY *(Leave blank)*	2. REPORT DATE	3. REPORT TYPE AND DATES COVERED
	6/15/97	Final Report 4/15/97 to 5/15/97

4. TITLE AND SUBTITLE

Multi-Parameter Snow Sounding Probe

5. FUNDING NUMBERS

DAAG55-97-C-0013

6. AUTHOR(S)

Robert L. Foster, Dr. Michel Louge, et.al.

7. PERFORMING ORGANIZATION NAME(S) AND ADDRESS(ES)

Capacitec, Inc.
87 Fitchburg Rd.
Ayer, MA 01432 USA

8. PERFORMING ORGANIZATION REPORT NUMBER

9. SPONSORING/MONITORING AGENCY NAME(S) AND ADDRESS(ES)

U.S. Army Research Office
P.O. Box 12211
Research Triangle Park, NC 27709-2211

10. SPONSORING/MONITORING AGENCY REPORT NUMBER

ARO 36672.1-GS-SBI

11. SUPPLEMENTARY NOTES

The views, opinions and/or findings contained in this report are those of the author(s) and should not be construed as an official Department of the Army position, policy, or decision, unless so designated by other documentation.

12a. DISTRIBUTION/AVAILABILITY STATEMENT

Approved for public release; distribution unlimited.

12b. DISTRIBUTION CODE

13. ABSTRACT *(Maximum 200 words)*

We describe a penetration field-portable capacitance probe capable of recording profiles of dielectric permittivity through the snow pack. The probe was developed under the auspices of the Army Research Office as a Phase I SBIR project. It consists of a wedged capacitance tip, which is mounted at the end of a pole allowing its penetration through depths of at least 2 m. The capacitance instrument is integrated in the tip. By appropriate placement of its ground, guard and sensor conductive surfaces, the probe sheds horizontal electric field lines permitting it to resolve horizontal snow layers of 2.5 mm

continued on reverse side

DTIC QUALITY INSPECTED 4

14. SUBJECT TERMS		15. NUMBER OF PAGES
Snow pack	Per table probe	31
Capacitance probe	snow density	16. PRICE CODE
Snow dielectric permittivity	snow wetness	

17. SECURITY CLASSIFICATION OF REPORT	18. SECURITY CLASSIFICATION OF THIS PAGE	19. SECURITY CLASSIFICATION OF ABSTRACT	20. LIMITATION OF ABSTRACT
UNCLASSIFIED	UNCLASSIFIED	UNCLASSIFIED	UL

"A Portable Capacitance Snow Sounding Probe"

SBIR Phase I Final Report

by

Robert L. Foster
Capacitec, Inc.
PO Box 819
87 Fitchburg Road
Ayer, MA 01432

and

Michel Y. Louge
Sibley School of Mechanical and Aerospace Engineering
Cornell University
Upson Hall
Ithaca, NY 14853 USA

19970819 018

Abstract

We describe a penetration field-portable capacitance probe capable of recording profiles of dielectric permittivity through the snow pack. The probe was developed under the auspices of the Army Research Office as a Phase I SBIR project. It consists of a wedged capacitance tip, which is mounted at the end of a pole allowing its penetration through depths of at least 2 m. The capacitance instrument is integrated in the tip. By appropriate placement of its ground, guard and sensor conductive surfaces, the probe sheds horizontal electric field lines permitting it to resolve horizontal snow layers of 2.5 mm thickness. Signal processing is achieved with a lightweight, hand-held, autonomous amplifier featuring simple controls, memory, and a RS-232C interface.

The probe was tested at the mountain resort of Alta near Salt Lake City, Utah. There, it recorded the real and imaginary parts of the snow dielectric constant through a typical winter snow pack. Using independent calibrations, measurements of the dielectric modulus provided an accurate profile of snow density. In addition, the vertical record of the imaginary part clearly revealed the presence of ice layers that were later confirmed by the excavation and interpretation of a detailed snow cover profile.

Introduction

In a workshop organized by the US Army Research Office in October 1995, the snow science community assigned its highest priority to the development of a multi-parameter snow penetration probe capable of recording physical parameters governing the mechanical properties of the snow pack (Brown and Dent, 1996). The recommendation was inspired by the report of Dr. Hansueli Gubler, a leading instrumentation scientist, and by the recent application of capacitance techniques to the measurement of snow density and velocity by a group from Cornell University, Montana State University, the University of Utah and the Swiss Federal Institute for Snow and Avalanche Research. Among the desired parameters (density, temperature, grain size, wetness and cohesion), the suggestion was to begin with a capacitance measurement of dielectric permittivity to infer density and wetness (Dozier, 1996; Colbeck, 1978; Boyne and Fisk, 1987).

Vertical soundings of the snow pack are essential diagnostic tools for snow hydrologists and avalanche forecasters. The hydrologists require relatively quantitative profiles of snow density from which they can infer the total amount of snow coverage in a region. Because they generally inspect the snow pack long after precipitation, their snow is often dense and fully settled. Because variations in altitude and terrain can result in widely different coverage, they must dig a relatively large number of pits for accurate predictions of total snow fall. Avalanche forecasters, on the other hand, are concerned with more recent precipitation and relatively rapid

metamorphosis of buried snow layers. While they too require a relatively large number of pits to assess the avalanche potential of a basin, they often perform a more qualitative inspection aimed at identifying the presence and depth of weak layers in a relatively immature snow pack.

In this context, we have developed a penetration field-portable capacitance probe capable of recording profiles of dielectric permittivity through the snow pack. The idea is to acquire density profile data without the need for excavation. The probe consists of a pole with a wedged capacitance tip allowing penetration through depths of at least 2 m. The capacitance tip is connected to a hand-held amplifier for data processing and storage.

The probe was tested at the mountain resort of Alta in cooperation with the University of Utah, the Utah Department of Transportation and the Center for Snow Science at Alta. There, it recorded the real and imaginary parts of the snow dielectric constant through a typical winter snow pack. Using independent calibrations, measurements of the dielectric modulus provided an accurate profile of snow density. In addition, the vertical record of the imaginary part clearly revealed the presence of ice layers that were later confirmed by the excavation and interpretation of a detailed snow cover profile.

After providing some background on capacitance snow instrumentation, the present report describes the design of the sounding probe and outlines the tests carried out at Alta. A user's manual for the probe is included in an Appendix.

Background

This section summarizes the principle of our processing electronics and the dielectric properties of typical snows.

Processing electronics

As Fig. 1 illustrates, generic capacitance probes consist of three conductors called the "sensor", "ground" and "guard" electrodes. The electronics records the impedance Z between sensor and ground, while a buffer amplifier maintains the guard at precisely the same sinusoidal voltage as the sensor's. Because it absorbs distortions of the electric field caused by external interferences, the guard protects the sensor from stray capacitances. In addition, because the sensor is connected to the processing circuits using a guarded coaxial cable, the cable capacitance does not participate in the measurement. By eliminating stray and cable capacitances, the technique can detect capacitances three to six orders of magnitude smaller than conventional bridges of similar cost. Note that, because our exact implementation of the circuit shown in Fig. 1 is proprietary, details are not provided in the present report.

To ensure proper operation of the guard electrode, the electronics must maintain the guard voltage v_g equal to the sensor voltage v_s. This is accomplished by sampling v_s through a buffer amplifier of unity gain. This buffer has a suitably high input impedance to avoid disturbing the sensor circuit. Further protection of the sensor circuit from external interferences is accomplished by surrounding it with a guarded shield. The output of the system is the rectified guard voltage V, which the buffer keeps proportional to the amplitude of the sensor voltage.

Another objective of the electronics is to pass a sinusoidal current of constant amplitude through the test impedance Z. To this end, the carrier oscillator generates a voltage v_r of constant, albeit user-adjustable, amplitude. The amplitude of the sensor current i is kept constant by controlling the voltage $(v_s - v_1)$ across the reference impedance Z_r. This is achieved by sampling the sensor voltage v_s through the buffer, adding the difference $(v_s - v_1)$ to the oscillator voltage, and feeding the result to the reference impedance through an amplifier of high gain H (Fig. 1).

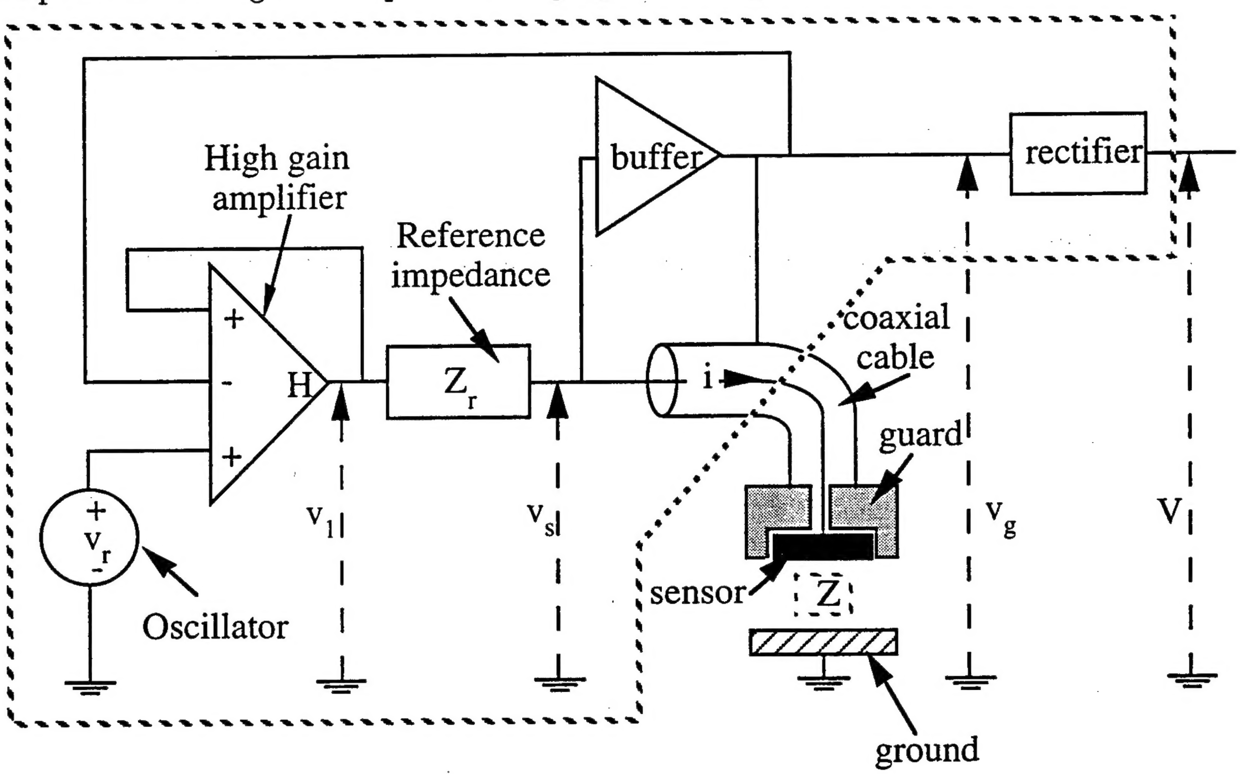

Fig. 1. Schematic of the electronic system. The dashed lines represent the physical boundary of the processing circuits. Z is the impedance between sensor and ground.

Assuming negligible current input into the amplifiers, the voltage v_1 into the reference impedance is

$$v_1 = H\,(v_r - v_g + v_1) = i\,(Z_r + Z)\,, \tag{1}$$

while the guard voltage is

$$v_g = v_s = Z\, i. \tag{2}$$

Eliminating v_1 from Eqs. (1) and (2) yields

$$\frac{v_r}{v_g} = \frac{1}{H} + \frac{Z_r}{Z}\left(\frac{1-H}{H}\right) \tag{3}$$

and

$$i = \frac{v_r}{Z_r}\left(\frac{1}{\left(\frac{Z}{Z_r}\right)\left(\frac{1}{H}\right) + \left(\frac{1-H}{H}\right)}\right). \tag{4}$$

Because H is large and real, inspection of Eq. (4) indicates that the current is nearly independent of Z,

$$i \approx - v_r/Z_r\,, \tag{5}$$

and the modulus of Eq. (3) is, to a good approximation,

$$\frac{|v_r|}{|v_g|} \approx \frac{|Z_r|}{|Z|}. \tag{6}$$

Because rectification produces a voltage proportional to v_g, the output V is itself proportional to the modulus of Z.

For media with negligible imaginary part of the permittivity, $Z = 1/j2\pi fC$, where f is the frequency of the oscillator and $j^2=-1$. In this case, the system produces a rectified output voltage that is related to C, the capacitance between the ground and sensor surfaces, through the empirical relation

$$V = Q_s/gC, \tag{7}$$

where Q_s is a system constant and g is an adjustable gain parameter. From Eq. (7), the effective dielectric constant ε_e of a homogeneous suspension covering the probe is obtained by forming the ratio of V_0, the rectified probe output in air, and V, the output in the presence of the dielectric powder of interest,

$$\varepsilon_e \equiv C/C_0 = V_0/V, \tag{8}$$

where C_0 is the probe capacitance in air. For a dielectric powder, it remains to infer the volume fraction from the measurement of ε_e. This is achieved by analyzing or calibrating the dielectric behavior of the suspension (Louge and Opie, 1990).

For media like snow with a significant imaginary part of the permittivity, the voltage ratio V_0/V yields the modulus of Z,

$$\frac{V_0}{V} = \left|\frac{Z_0}{Z}\right| = \frac{1}{2\pi f\, C_0\, |Z|}, \tag{9}$$

where Z_0 is the probe's impedance in air. For isotropic media, the electric displacement D and the electric intensity E are colinear vectors; however,

because they are not generally in phase, the effective dielectric constant ε_e may exhibit real and imaginary parts,

$$\varepsilon_e \equiv D/\sigma_0 E = \varepsilon' - j\,\varepsilon'' , \tag{10}$$

where ε' and ε'' are both functions of frequency and $\sigma_0 = 8.854\ 10^{-12}$ F/m is the dielectric permittivity of free space and, to a good approximation, of air. The corresponding impedance between sensor and ground is

$$Z = \frac{1}{\ell\, 2\pi f\, \sigma_0\, (\varepsilon'' + j\varepsilon')} . \tag{11}$$

In this expression, ℓ is a characteristic length of the capacitance probe geometry,

$$\ell \equiv C_0/\sigma_0 . \tag{12}$$

In the presence of a homogeneous, isotropic suspension, ℓ is independent of ε_e. Thus, from Eqs. (9) through (12), the voltage ratio yields the modulus of ε_e,

$$\frac{V_0}{V} = \sqrt{\varepsilon''^2 + \varepsilon'^2} . \tag{13}$$

In order to resolve both components of ε_e, we exploit the phase lag ϕ between v_r and v_g, which are both readily available for measurement. From Eq. (3),

$$\tan\phi = \frac{1 - \dfrac{m}{n}\dfrac{\varepsilon'}{\varepsilon''}}{\dfrac{\varepsilon'}{\varepsilon''} + \dfrac{m}{n} + \dfrac{1}{2\pi f\, \sigma_0\, \varepsilon''\, \ell\; n(1+H)}} . \tag{14}$$

where m and n are the real and imaginary parts of the conjugate of Z_r,

$$Z_r \equiv m - n\,j . \tag{15}$$

In general, the constants m/n and n(1+H) are found by recording ϕ for a series of known capacitances. When our processing electronics operates at 16 kHz amplifier, Z_r is purely capacitive, so m = 0. Note that, in order to permit successful measurements of capacitance in air, the condition

$$|\, 2\pi f\, \sigma_0\, \ell\; n(1 - H)\,| >> 1 \tag{16}$$

must be satisfied to let Eq. (6) be a valid approximation of Eq. (3). Consequently, at 16 kHz with m = 0, Eq. (14) reduces to

$$|\tan\phi| \approx \frac{\varepsilon''}{\varepsilon'} , \tag{17}$$

so, at this frequency, the phase lag between v_r and v_g is a direct measure of the "loss tangent" ($\varepsilon''/\varepsilon'$). If both real and imaginary parts of ε_e are required,

frequencies, the determination of ε' and ε" requires a more complicated solution involving Eqs. (13) and (14) and the knowledge of ℓ for the probe.

For the present technique, we follow others (eg, Kuroiwa, 1967; Denoth, et al, 1984) in assuming that the snow sample contained in the probe's measurement volume is sufficiently isotropic and homogeneous to possess an effective dielectric constant satisfying Eq. (10). Then it remains to evaluate this constant through calibration.

Dielectric properties of snow

The principal challenge of capacitance techniques is to infer density and wetness from the measurements of ε' and ε". As Fig. 2 illustrates, most snows of practical interest behave as a Debye dielectric above a minimum oscillator frequency f_0. In this case, the real and imaginary parts of the permittivity fall on a "Cole-Cole" circle where

$$\varepsilon_e = \varepsilon' - j\,\varepsilon'' = \varepsilon^e_\infty + \frac{\varepsilon^e_0 - \varepsilon^e_\infty}{1 + j\,2\pi f\,\tau}\,. \tag{18}$$

In this expression, ε^e_0 and ε^e_∞ are the limits of ε' at vanishing and infinite frequencies and τ is the relaxation time of electric displacement.

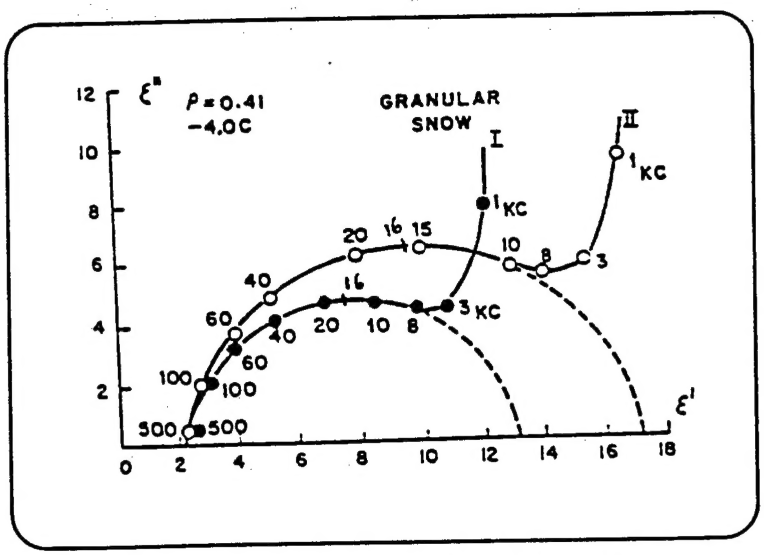

Fig. 2. Imaginary part versus real part of the dielectric constant of granular snows (after Kuroiwa, 1967). For each point, frequency is shown in kHz. Semi-circles are best fit "Cole-Cole" circles from Eq. (2).

To a good approximation, ε^e_∞ grows linearly with snow density ρ and quadratically with volumetric liquid-phase water content W (Denoth, et al, 1984); for example, for wet alpine snow,

$$\varepsilon_\infty^e \approx 1 + 2.2\,\rho + 0.19\,W + 0.005\,W^2. \tag{19}$$

Because it is nearly independent of temperature and snow type and texture, ε_∞^e produces a robust measurement at frequencies above 10 MHz. Unfortunately, because proper guiding of such radio or microwave frequencies limits the instrument's spatial resolution to distances of order the wavelength $\lambda \sim c / f\,(\varepsilon_\infty^e)^{1/2}$, an instrument using microwave frequencies cannot distinguish narrow structures of the snow pack. In addition, it is difficult to implement a guarded circuit under these conditions. As Fig. 1 suggests, proper operation of the buffer requires that the capacitive impedance $1/2\pi fjC_{sg}$ between sensor and guard be large enough not to interfere with the buffer's operations. Frequencies above 10 MHz generally fail to satisfy this criterion with cables of reasonable lengths. Consequently, measurements with guarded capacitance probes are limited to lower frequencies, unless one forgoes the convenience of the coaxial cable and locates the processing electronics near the probe head.

Because for most snows the minimum Debye frequency f_0 is typically 10 kHz for most snows and generally no greater than 20 kHz, an alternative idea is to infer the optical dielectric constant ε_∞^e from sweeping oscillator frequency in the range 10 to 100 kHz.

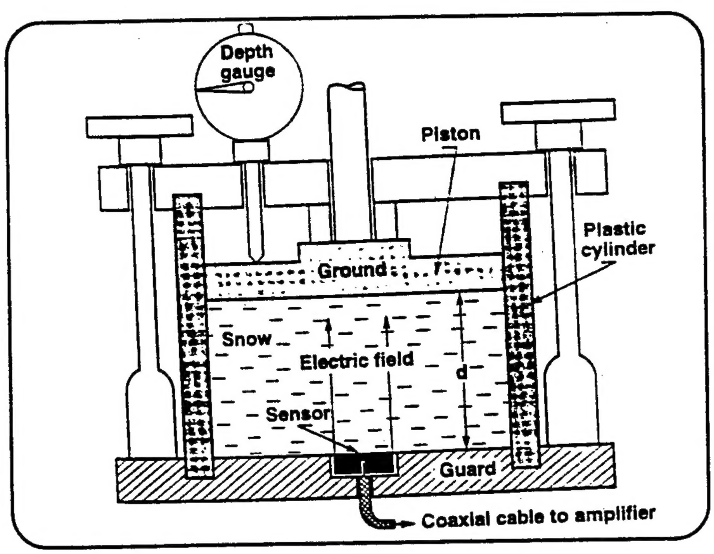

Fig. 3. The "snow press."

At the much lower frequency of 16 kHz, Louge, et al (1997) evaluated the dielectric constant of various snow samples using the capacitance instrument sketched in Fig. 3. This "snow press" included a grounded piston traveling in a plastic cylinder of 102 mm diameter. The base featured a circular sensor surface surrounded by a guard plate. Once a sample was

introduced in the press, the piston was progressively lowered to bring it to denser compactions while the corresponding values of ε_e were measured.

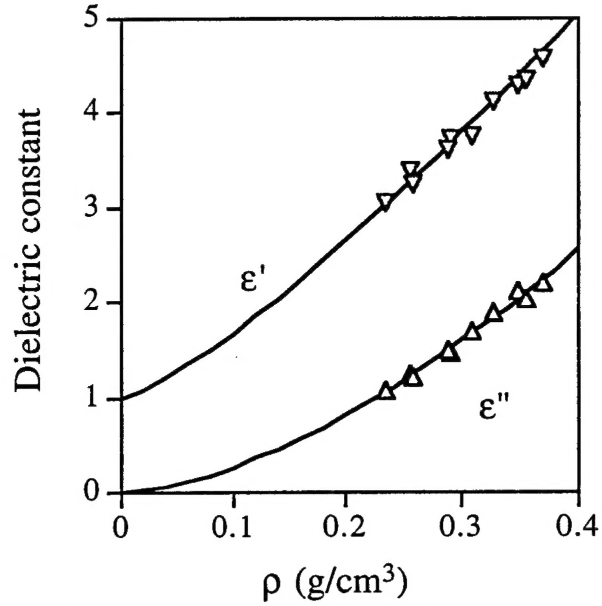

Fig. 4. Dielectric permittivity of fresh Montana snow at -8.8°C.

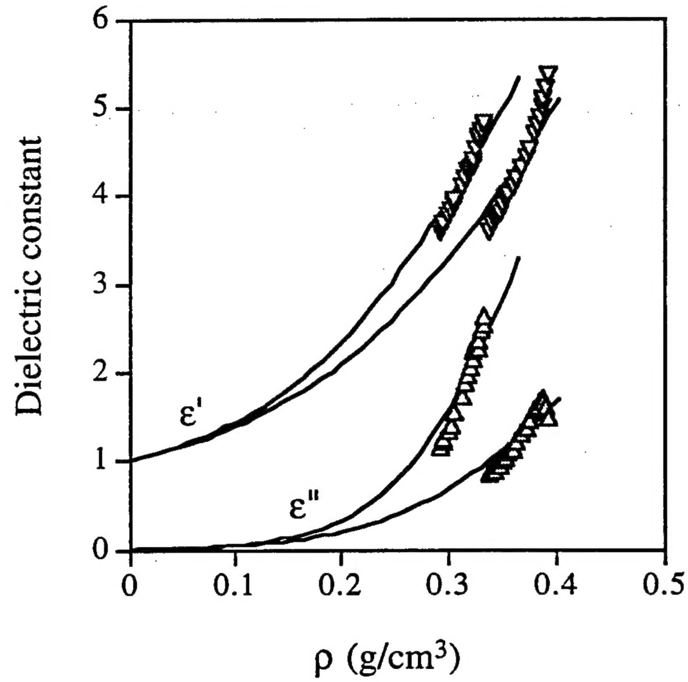

Fig. 5. Dielectric properties of ice grains of 1mm mean size observed in Davos at -7°C (open symbols) and -9°C (solid symbols).

To drive the "snow press" and other capacitance instruments, Louge, et al (1997) exploited our standard electronics operating at 16 kHz. Because at this frequency $|\varepsilon_e|$ is considerably larger than ε_∞^e, the capacitance measurement was more sensitive to snow density than at radio frequencies.

The presence of liquid-phase water or impurities further raised the values of ε'', and to a lesser extent, ε' (Kuroiwa, 1967). At 16kHz, Louge, et al distinguished two broad categories of snow response. The first was exhibited by relatively light, dry, crystalline snows (Fig. 4). The second broad category of snow behavior was represented by irregular faceted ice grains (Fig. 5). For all snows, both real and imaginary parts of ε_e increased with density.

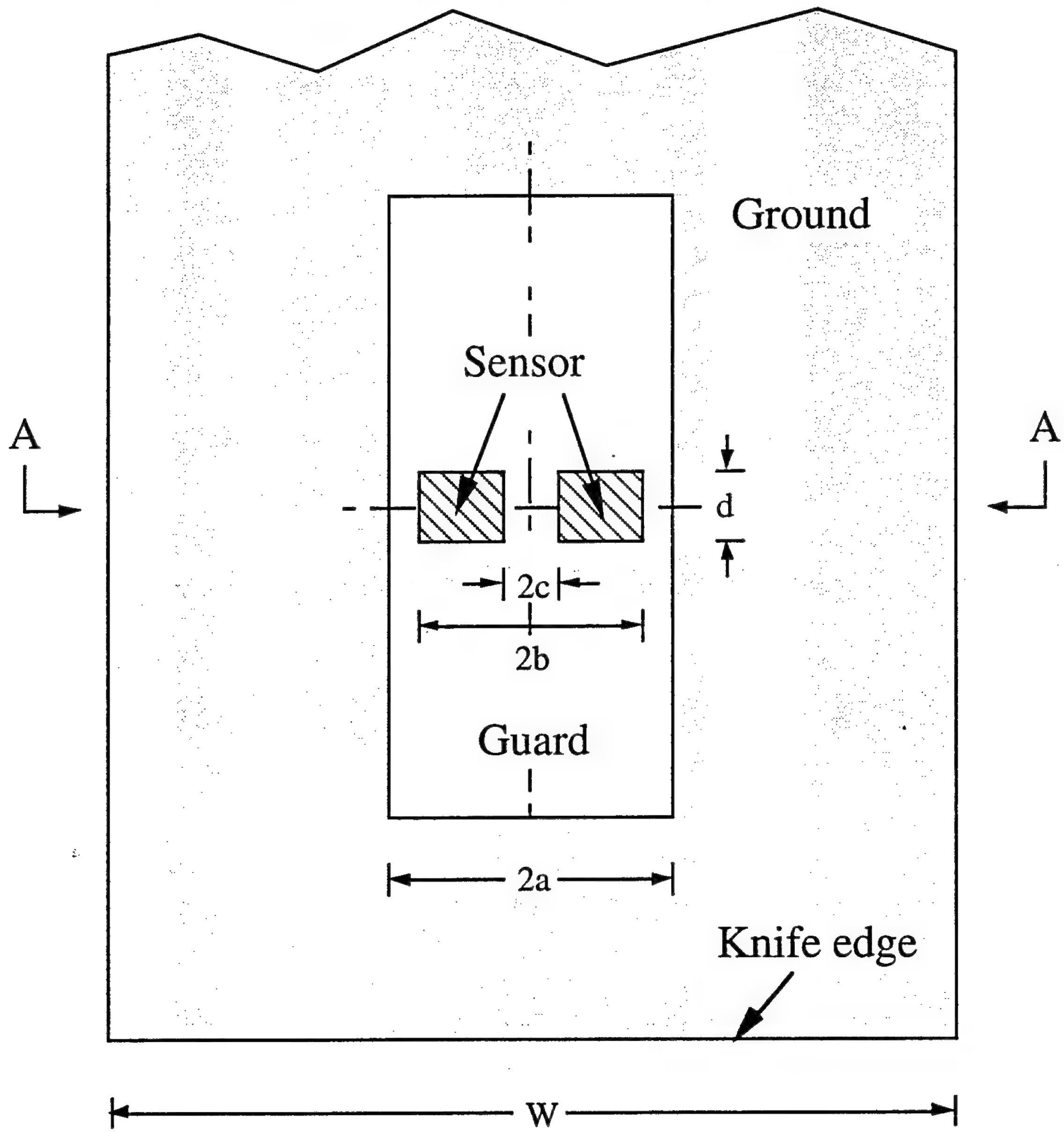

Fig. 6. Front view of the probe face. Dimensions are not to scale.

Probe Design

The probe tip is sketched in Fig. 6. It is mounted at the end of a pole allowing its penetration through depths of at least 2 m. Its sensor consists of two rectangular conductive surfaces located on either side of the vertical axis

of symmetry and surrounded by a relatively wide guard. In a homogeneous medium, this placement permits the sensor to shed largely horizontal circular field lines bounding a measurement volume of height equal to that of the sensors. To illustrate the design, we now derive the capacitance of the probe in air and the height of the measurement volume.

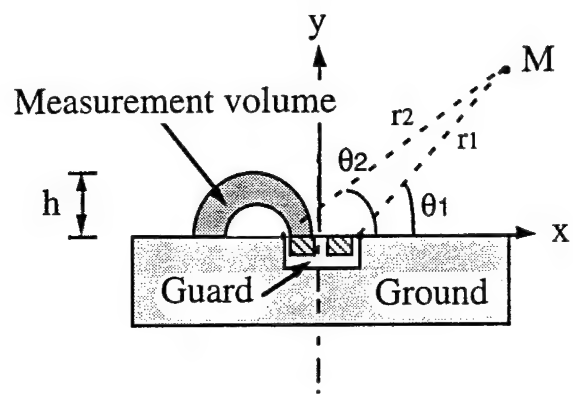

Fig. 7. Section AA showing measurement volume and notation. In this two-dimensional configuration, the section can be represented as the complex plane. Voltage singularities are located between guard and ground.

Figure 7 is a sketch of the quasi-two dimensional electric field emanating from the sensors. Because the frequency of the oscillator is small, the field Eq. has negligible unsteady terms. It further reduces to the Laplace Eq. in the absence of free charges in the suspension. Because the Laplace Eq. is linear, the identical excitation of guard and sensor may be treated as a voltage of fixed amplitude $\tilde{V}$ over the entire guard/sensor assembly. In this case, voltage singularities are located at the boundary between the ground and the guard/sensor assembly (Fig. 7). For this symmetric configuration, it is instructive to derive the electric field near the probe from two-dimensional complex solutions of the Laplace Eq. For simplicity, we consider a two-dimensional homogeneous medium above two adjacent equipotential surfaces held at different voltages. The first surface represents the guard/sensor assembly. The second surface is the ground. In this analysis, we ignore the thin dielectric layer that insulates the three electrodes from one another. The complex function that satisfies the conditions $v = \tilde{V}$ for $x \in]-a,+a[$ and $v = 0$ elsewhere is

$$\Phi = \frac{\tilde{V}}{\pi}\left([\theta_1-\theta_2] + j\ln\left(\frac{r_2}{r_1}\right)\right), \tag{20}$$

where the angles and radii are shown in Fig. 7. The corresponding voltage distribution is

$$v = (\tilde{V}/\pi)\,(\theta_1 - \theta_2)\,. \tag{21}$$

On an electric field line, the imaginary part of Φ and, consequently, the ratio r_2/r_1, are constant. The field lines are therefore a family of circles of radius R with center located on the axis at an abscissa x_c satisfying

$$(R/a)^2 + (x_c/a)^2 = 1\,. \tag{22}$$

The electric field arising from the complex potential Φ is

$$\mathbf{E} = -\nabla v\,, \tag{23}$$

and the magnitude of $\mathbf{E}$ at the wall determines the charge distribution there,

$$\mathbf{E} = (\xi / \sigma_0)\,\mathbf{n}\,, \tag{24}$$

where ξ is the charge surface density and $\mathbf{n}$ is the outward normal to the plane. Combining (21), (23) and (24) yields the charge density for $x \in\,]-a,+a[$

$$\xi = \frac{\tilde{V}\sigma_0}{\pi}\left(\frac{1}{x+a} - \frac{1}{x-a}\right). \tag{25}$$

Upon integrating this density distribution, the total charge on the sensor surface and, consequently, the probe capacitance in air may be calculated. We find

$$C_0 = \frac{2\,d\,\sigma_0}{\pi}\,\ell n\left[\frac{a+b}{a-b}\,\frac{a-c}{a+c}\right], \tag{26}$$

or, equivalently,

$$\ell = \frac{2\,d}{\pi}\,\ell n\left[\frac{a+b}{a-b}\,\frac{a-c}{a+c}\right]. \tag{27}$$

This calculation also allows us to estimate the height of the measurement volume, which, in a homogeneous medium, is bounded by the extreme field lines emanating from edges of the sensor surfaces. From Eq. (22), the height of the outermost field line is

$$h = (a^2 - c^2)/2c\,. \tag{28}$$

Because, as this Eq. indicates, increasing the dimension c reduces h, it is natural to bring the edge of the sensor surface closer to the singularities at $x = \pm a$ in order to confine the measurement volume further. However, increasing c makes it more difficult to control the value of the capacitance. In the extreme situation where b and c nearly equal a, the value of the capacitance is very difficult to predict, as it becomes excessively sensitive to small excursions in the values of c/a and b/a. The simple sensitivity analysis that follows captures this effect.

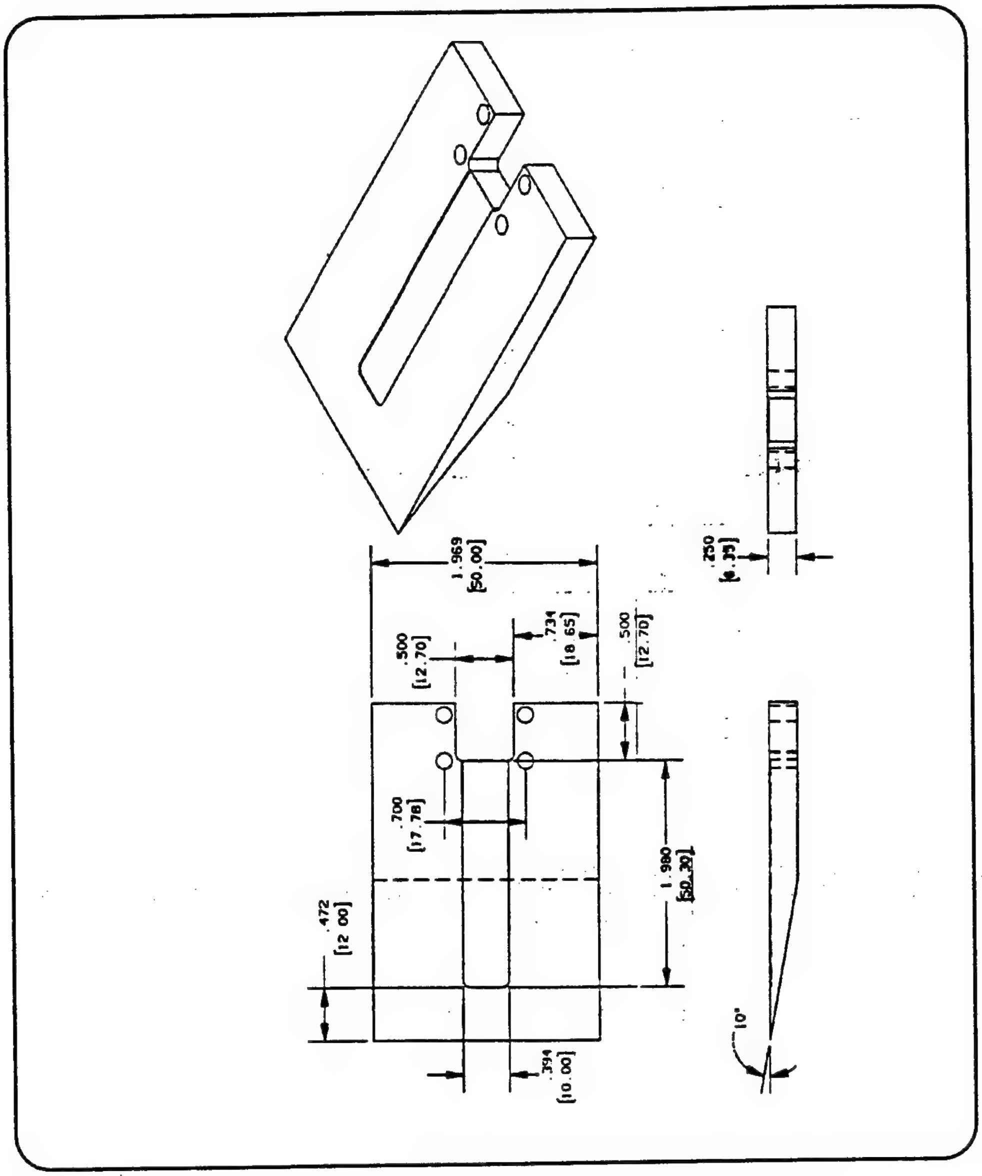

Fig. 8. Perspective drawing of the probe head.

First, we estimate the relative uncertainties in the capacitance by differentiating Eq. (26) with respect to b and c. Assuming that the uncertainties Δb and Δc are statistically uncorrelated, but equal to a common tolerance δ, we find

$$\frac{\Delta C_0}{C_0} = \left(\frac{\delta}{a}\right)\left\{\frac{2}{\ln\left[\left(\frac{1+b/a}{1-b/a}\right)\left(\frac{1-c/a}{1+c/a}\right)\right]}\sqrt{\frac{1}{[1-(b/a)^2]^2}+\frac{1}{[1-(c/a)^2]^2}}\right\}. \qquad (29)$$

For any given value of (c/a), we find that this expression is minimum for a unique value of (b/a) i.e.,

$$\left(\frac{b}{a}\right)_{optimum} \approx 0.29 \left(\frac{c}{a}\right) + 0.70 \tag{30}$$

Further, we find that $\Delta C_0/C_0$ decreasing with decreasing (c/a). Because (c/a) must be large enough to permit adequate clearance between the two sensors, our design strategy is to prescribe (c/a) = 0.2 and, according to Eq. (30), to set (b/a) ≈ 0.76 to minimize the sensitivity of the capacitance to excursions in probe dimensions that may result, for example, from manufacturing tolerances or deterioration of the front probe surface.

Thus, in the prototype of our sounding probe, we use a = 5 mm, b = 4 mm and c = 1 mm. The corresponding characteristic capacitance length of the probe is then ℓ = 2.8 mm in air. Figure 8 is the corresponding perspective drawing of the probe head.

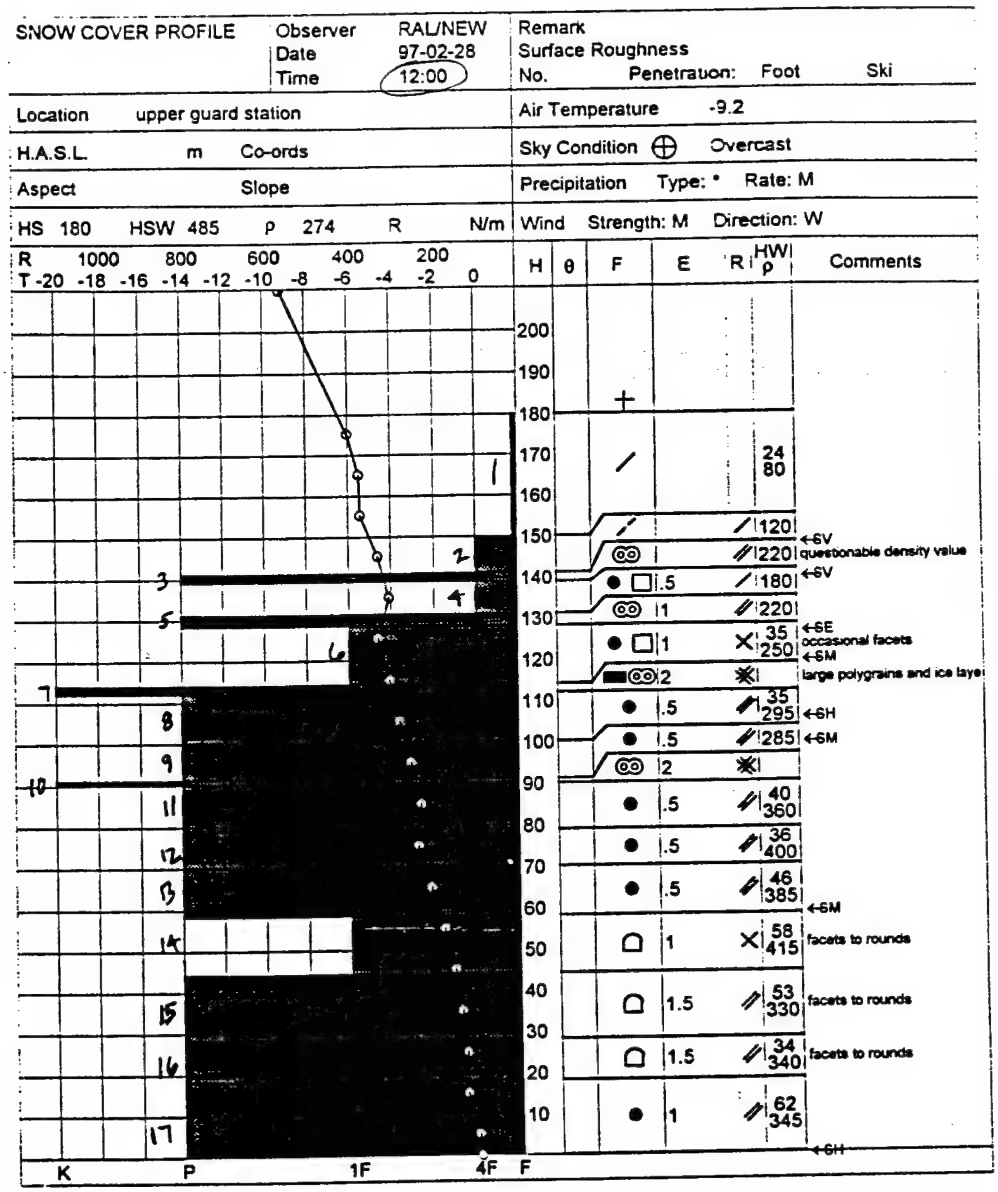

SNOW COVER PROFILE	Observer RAL/NEW Date 97-02-28 Time 18:00	Remark Surface Roughness No. Penetration: Foot Ski
Location Upper Guard		Air Temperature -11.2
H.A.S.L. m Co-ords		Sky Condition
Aspect Slope		Precipitation
HS 180 HSW ρ R -173 N/m		Wind

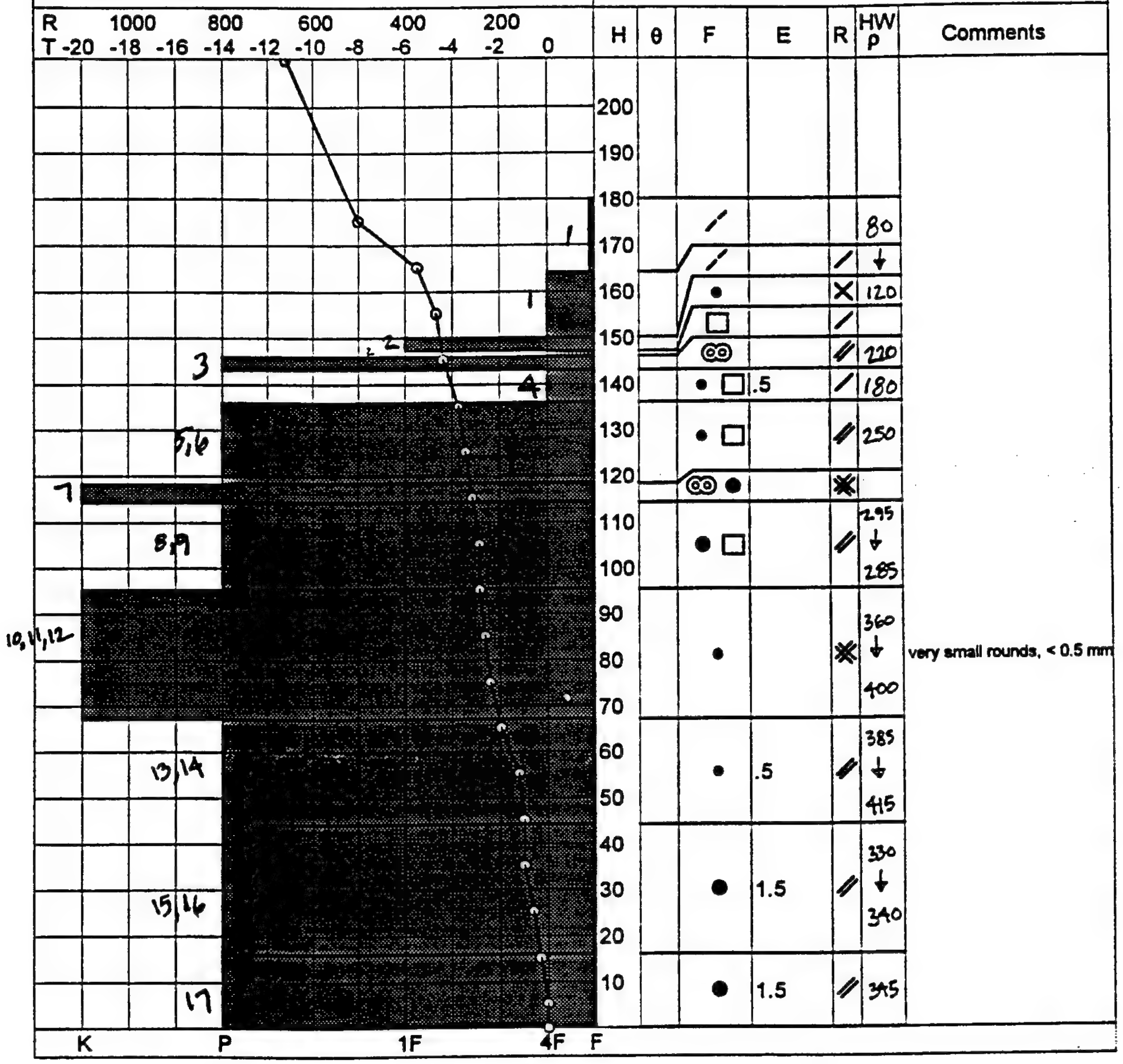

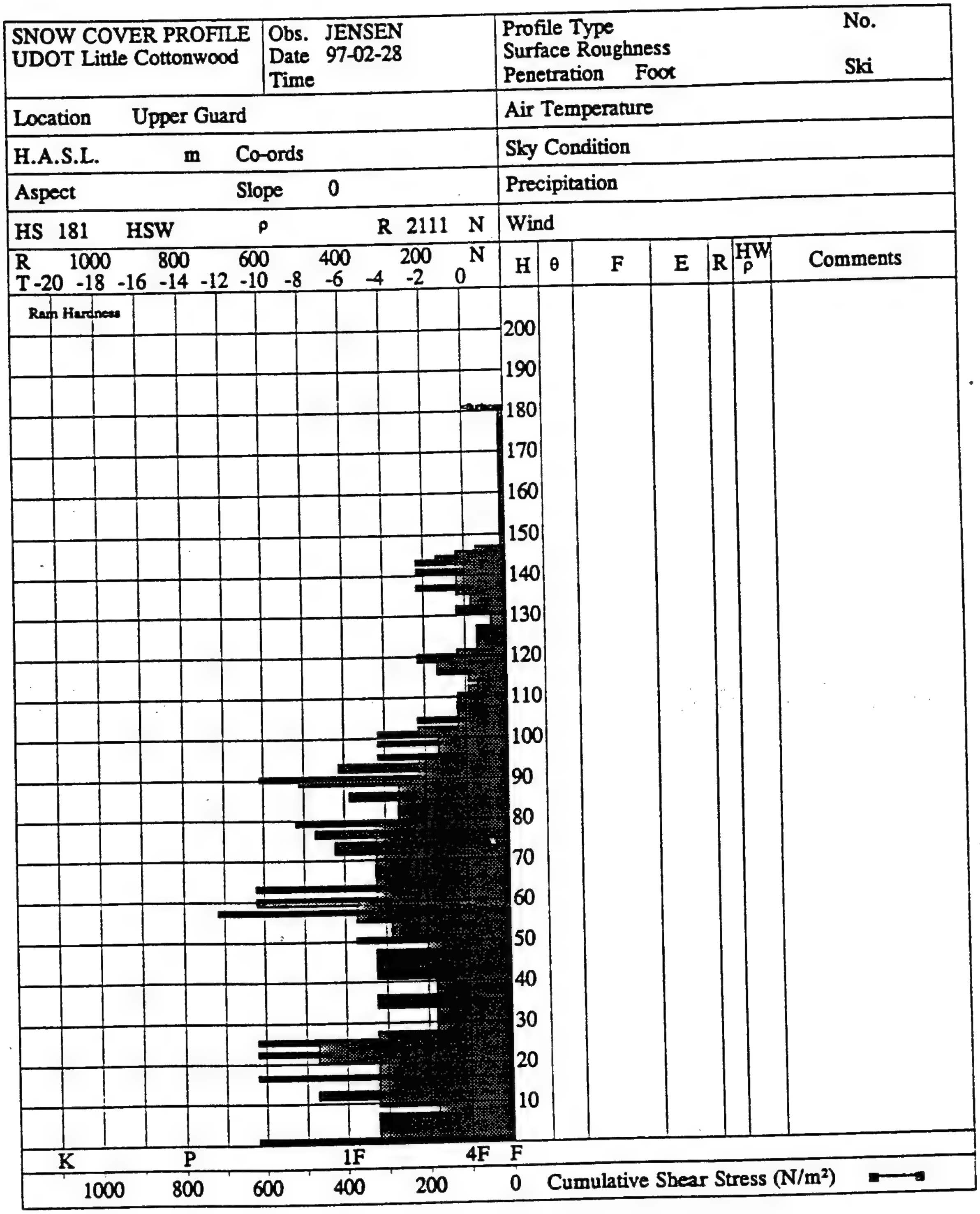

Fig. 9. Snow profiles obtained on February 28 at (a) 12 noon and (b) 18:00; (c) ram penetrometer profile.

Field Tests

The probe was tested in the mountain resort of Alta near Salt Lake City, Utah. This section summarizes the conditions and results of the tests, which were carried out in cooperation with the University of Utah, the Utah Department of Transportation and the Center for Snow Science at Alta. We are particularly grateful to Professor Rand Decker and Mr. Daniel Howlett for putting us in touch with Messrs. Newel Jensen and Ralph Patterson, who provided logistical assistance and carried out complete snow profiles in an adjacent pit (Fig. 9).

Multi-frequency measurements

In the Alta tests, we first attempted measurements at several oscillator frequencies in the range 4 to 37 kHz with compact snow laid on the probe face. As outlined earlier, the idea was to exploit the Debye dielectric properties of snow to infer density and wetness from extrapolations of the Cole-Cole circle to high frequencies.

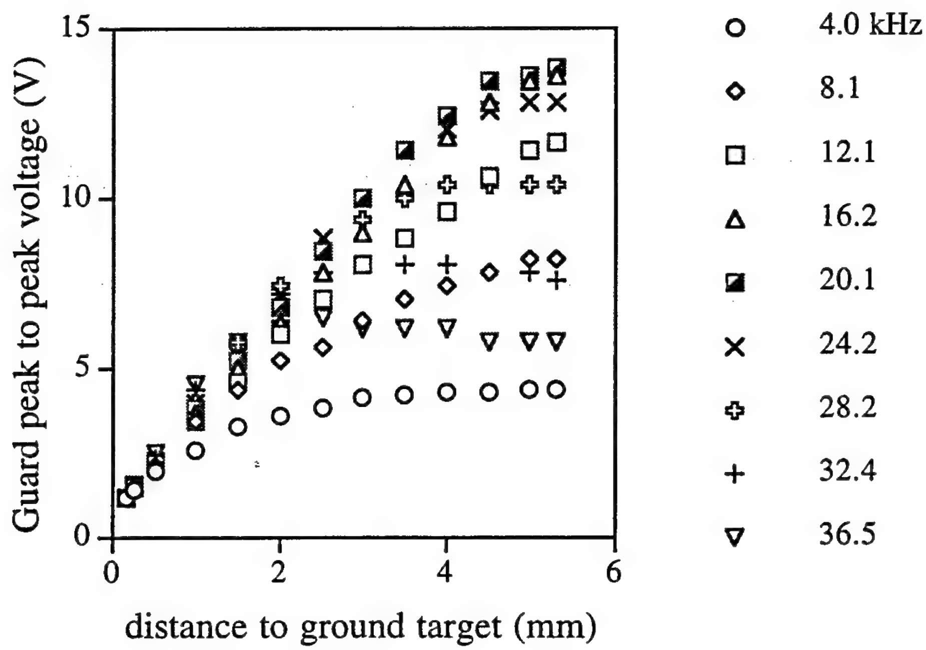

Fig. 10. Linearity tests of the portable amplifier for the amplifier frequencies shown in the legend in kHz. While frequencies between 16 and 24 kHz exhibit linear increase of the guard voltage over a wide range of distances, the voltage rolls off with distance at low or high frequencies.

Unfortunately, our attempts were complicated by non-linear behavior of the amplifier at frequencies other than its original 16 kHz design value. Figure 10 shows results of a test evaluating output linearity. In this test, the

probe is held parallel to a grounded target plate in air. When the plate and probe are separated by a distance of 5.3 mm, the corresponding capacitance is equal to that of the isolated snow probe in air. If the circuit was properly linear, the guard voltage would be directly proportional to the distance d between plate and probe face. As Fig. 10 indicates, linearity is best achieved at frequencies near 16 kHz. However, other frequencies exhibit roll-off that limits the corresponding amplifier linearity to a narrower range of capacitances. This behavior complicates data interpretation.

In these tests, we also recorded the phase lag between the oscillator and the guard. This permitted us to calculate the reference impedance Z_r (Eq. 15) at the frequencies of interest. We then exposed the probe face to snow cakes of controlled compaction and, knowing Z_r, we extracted both components of the snow dielectric constant from Eqs. (13) and (14). In Fig. 11, the resulting data is compared with pure snow in the Debye plane. As this Fig. shows, while trends are consistent with earlier observations, extrapolations are not accurate enough to fit a Cole-Cole circle through the points. The relatively small values of the ε'' recorded in our tests indicate that the snow samples were perhaps quite dry.

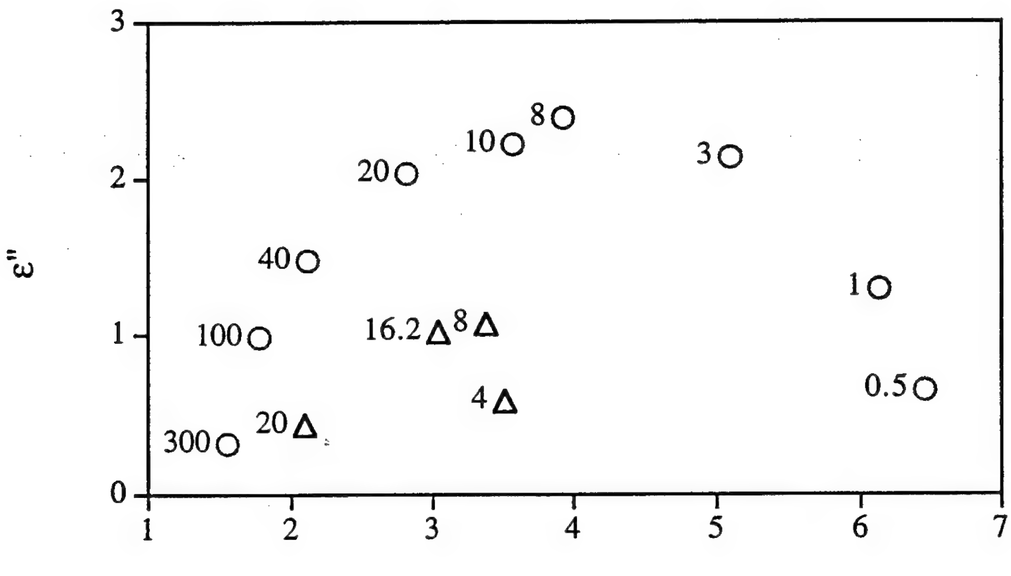

Fig. 11. Cole-Cole plot of imaginary versus real parts of the snow dielectric constant. The numbers shown are frequencies in kHz. Circles represent snow with $\rho = 0.26$ g/cm^3 at -8.5°C (from Kuroiwa, 1967). Triangles are tests of the capacitance probe with compacted fresh snow of $\rho = 0.28$ g/cm^3 at -7°C.

While it is relatively straightforward to solve the linearity problem of the probe amplifier at frequencies away from 16 kHz, we could not do so during the short time of the Phase I award. In this context, we can only

conclude that Cole-Cole extrapolations remain promising, as Camp and Labrecque (1992) have shown. As outlined in the next section, actual soundings at the optimum frequency of 16 kHz were far more conclusive.

Probe soundings

Figure 12 shows profiles of the real and imaginary parts of the dielectric constant acquired with the probe at 16 kHz. For this sounding, the probe was progressively inserted into the pack at 6 mm (1/4") intervals. Depth was recorded by marking the pole every quarter inch. Rather than pushing the probe in a continuous fashion, insertion was achieved by tapping the top of the pole until the net desired depth. This method permitted the greatest control of the sounding despite the variable strengths of successive snow layers.

To compare density measurements from the snow pit with the recorded capacitance sounding profiles, we first evaluated the dielectric properties of snows collected near the pit. To this end, we employed the "snow press" described by Louge, et al (1997). Figure 13 illustrates the corresponding calibrations. As expected from similar situations, faceted ice grains tended to exhibit larger values of the modulus of ε_e. The resulting fit permitted us to infer the snow density ρ from the soundings of $|\varepsilon_e|$. As Fig. 14 shows, the corresponding values of ρ are in excellent agreement with direct density measurements carried out in an adjacent pit.

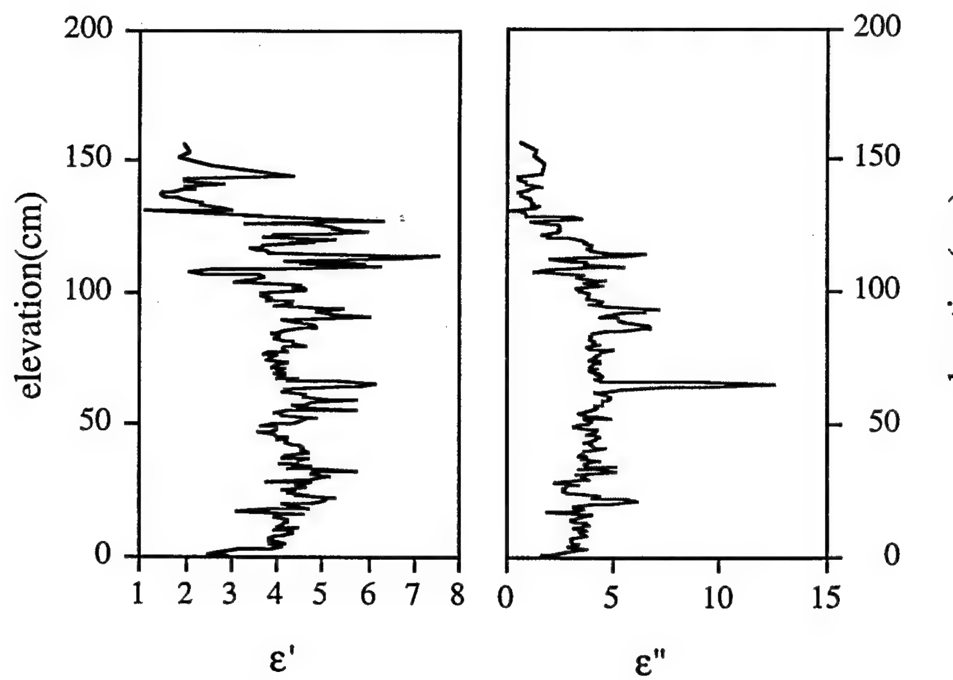

Fig. 12. Real and imaginary parts of the dielectric constant at 16 kHz versus elevation with origin is at the base of the pack.

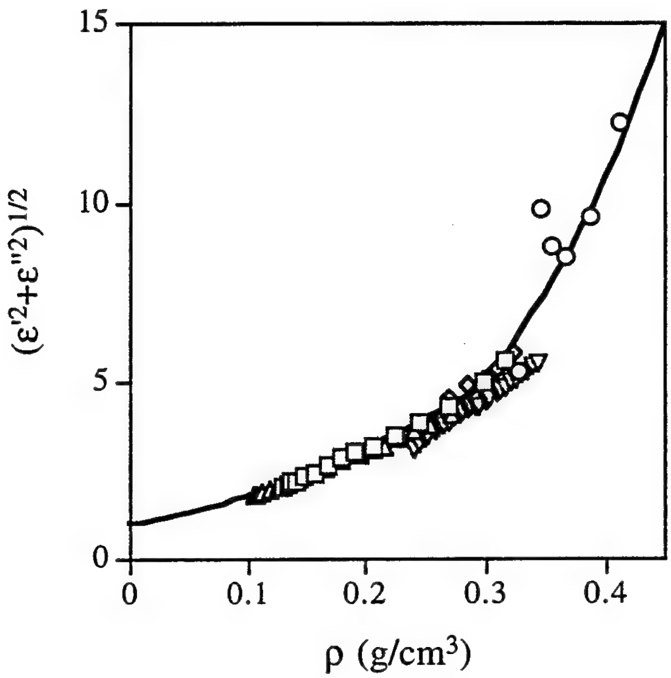

Fig. 13. Snow press calibration at 16 kHz of samples collected in the Alta snow pack. The best empirical fits are $\sqrt{\varepsilon'^2+\varepsilon''^2} \approx (\rho/\rho_0)^{1.5}$ for $\rho \leq 0.29$ g/cm^3 and $(\rho/\rho_1)^{3.1}$ for $\rho > 0.29$ g/cm^3, with $\rho_0 \approx 0.12$ g/cm^3 and $\rho_1 \approx 0.19$ g/cm^3.

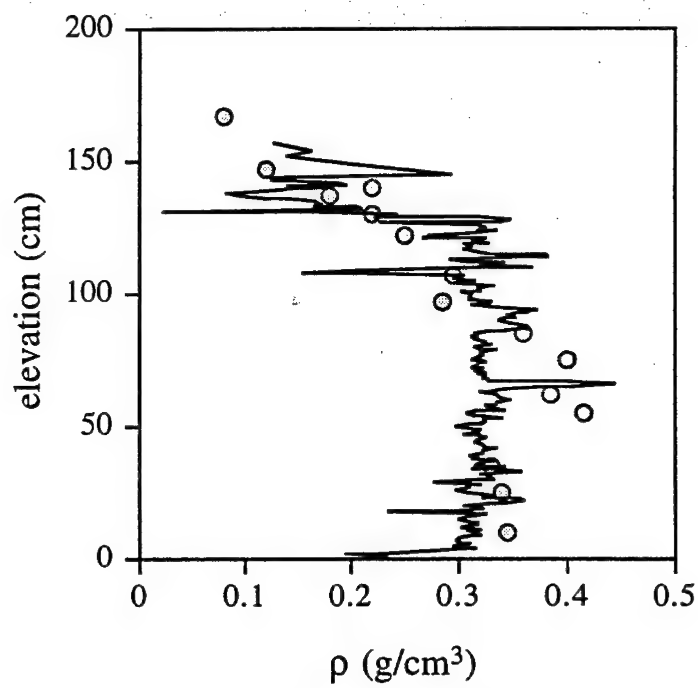

Fig. 14. Snow density versus elevation inferred from the sounding of Fig. 12 and the calibration of Fig. 13. The line is the detailed sounding of the capacitance probe and the symbols are from direct density measurements carried out in an adjacent pit (Fig. 9).

Because it permits rapid soundings with a narrow vertical spatial resolution, the capacitance probe records density profiles with greater detail or speed than the traditional excavation technique. Several noticeable features in Figs. 12 and 14 further illustrate advantages of the capacitance sounding method. Gradual compaction of fresh snow near the surface is well captured by the probe, followed by a sudden dip in the density. In the few centimeters above ground, the probe records a decrease in density that often corresponds to the local metamorphic depletion of grains near the warmer solid surface. This feature is too narrow to be captured by the pit profile. Other details appear on records of the complex components of ε_e. For example, an ice layer with large imaginary part ε'' clearly arises at 65 cm elevation. While largely undetected in the snow pit, the layer is visible on the ram penetrometer profile. Although further studies are needed to obtain a quantitative interpretation of both components of ε_e, it is promising that many detailed layers are observed in these records.

Future developments

The preliminary tests conducted at Alta suggest that our capacitance sounding probe is a viable alternative to the excavation of a pit for recording density profiles through the snow pack. Because snows gathered from a single basin are likely to exhibit similar dielectric properties, we envision the development and use of a field portable snow press that would permit rapid determination of the dependence of dielectric constant on density. Such calibration may obtained, for example, by rapidly extracting snow samples from a relatively crude pit. By connecting the press to our portable electronics, the latter can be programmed to incorporate calibration values automatically. Once such data is acquired, it is relatively straightforward to carry out any number of quantitative capacitance soundings from a region.

Another benefit of the probe is the apparent sensitivity of the imaginary part of the dielectric constant to the presence of ice layers and other inhomogeneities of the snow pack. While we have yet to demonstrate how extrapolating dielectric data over a range of frequencies can yield an independent measure of wetness, the idea is still promising enough to warrant further research.

In its present version, the probe is best used at a fixed frequency of 16 kHz. Although it relies on a calibration to produce quantitative density data, its soundings reveal the structure of the pack in considerable detail. Because of this success, we will consider commercializing the probe in its present state. Later, we hope to participate in further developments aimed at combining this probe with other instruments and to assist in the research to exploit its data further.

References

Boyne H.S. and Fisk D.J. (1987) "Comparison of snow cover liquid water measurement techniques," *Water Resources Research* **23**, 1833-36.

Brown R.L. and Dent J.D. (1996) "Research Priorities in Snow Mechanics and Snow Physics," *US Army Research Office.*

Camp P.R. and Labrecque D.R. (1992) "Determination of the Water Content of Snow by Dielectric Measurements," 92-18 Special Report AD-A256299, US Army Cold Regions Research and Engineering Laboratory, Hanover, NH, pp. 1-35.

Colbeck S.C. (1978) "Difficulties in measuring the water saturation and porosity of snow," *J. of Glaciology* **20**, 189-201.

Denoth A. , A. Foglar, P. Weiland, C. Mätzler, H. Aebischer, M. Tiuri and A. Sihvola (1984) "A comparative study of instruments for measuring the liquid water content of snow," *J. Appl. Phys.* **56** (7), 2154-2160.

Dozier J. (1996) "Optical and electric properties of snow," in Research Priorities in Snow Mechanics and Snow Physics, Brown R.L. and Dent J.D., eds., *US Army Research Office.*

Kuroiwa D. (1967) "Snow as a material. Chapter J. Electrical Properties of snow," in: Cold Regions Science and Engineering, Part II, Section B: Physical Sciences, US Army Materiel Command, Cold Regions Research and Engineering Laboratory, Hanover, NH, pp. 63-79.

Louge M. and M. Opie (1990) "Measurements of the effective dielectric permittivity of suspensions," *Powder Tech.*, **62**, 85-94.

Louge M.Y., Steiner R., Keast S.C., Decker R., Dent J. and Scheneebeli M. (1997) "Application of Capacitance Instrumentation to the Measurement of Density and Velocity of Flowing Snow," *Cold Regions Science and Technology*, **25**, 47-63.

APPENDIX

1. INTRODUCTION

The Multiparameter Snow Sounding System is a modified version of a Capacitec portable gap measuring electronics package. It incorporates a "toroidal style" capacitive probe, rulered 2 meter extendable snow "lance", and portable low capacitance electronic readout of permittivity and phase delay. There is also a 1000 point data logger, which eliminates the need for a portable PC in the field.

2. LAYOUT/PHYSICAL DESCRIPTION

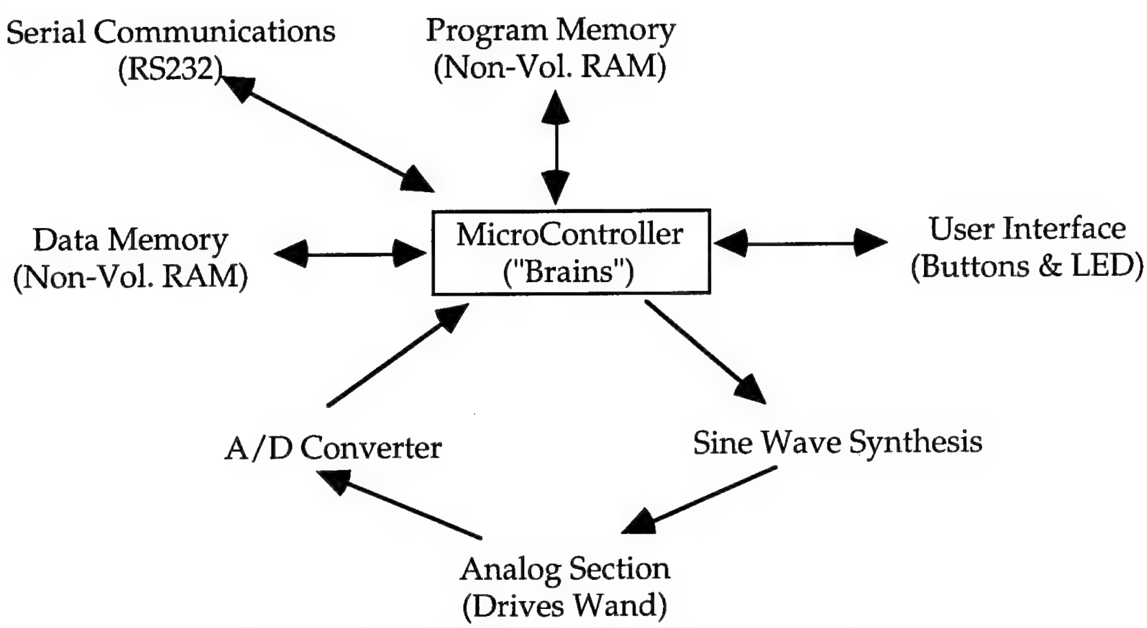

Figure 2.1. Snow Probe Functional Diagram.

Fig. 2.1 shows how the separate sections of the Snow Probe function together. The "brains" of the unit is the microcontroller, an 8-bit processor running with a 7MHz clock. It has access to 128K non-volatile memory (remains when power is off) for programming and data recording, a standard RS232 port for communicating with a PC, the interface section for user control and feedback, as well as the components that modulate and demodulate the signal on the wand.

2.1. Internal Components

The Snow Probe electronics contains four interconnected circuit boards that divide the tasks performed by the instrument. They are the microcontroller board, the power conversion board, the user interface board, and the sensor driver board. Each performs a specific set of tasks, described below.

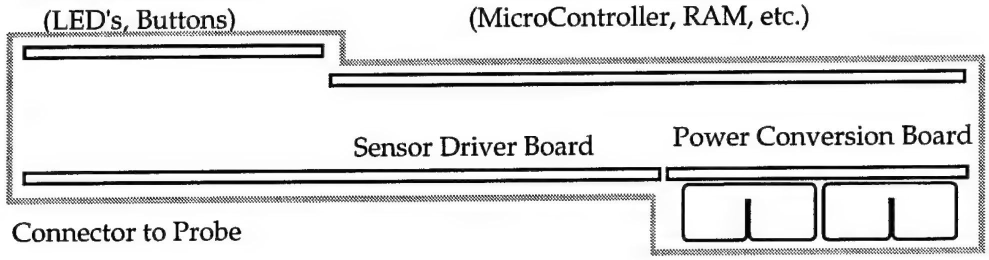

Figure 2.2 SnowProbe Electronics/Physical Layout (cutaway, side view).

2.1.1. MicroController Board

The microcontroller board contains a 68HC11 microcontroller operating at 7MHz, along with supporting non-volatile RAM, a clock/calendar chip, RS232 communications chips, and supporting digital circuitry. The board also contains an optional DAC (digital to analog converter) circuitry that can be used to synthesize analog voltage levels. This functionality is provided primarily for backward compatibility with analog input data recording equipment (data loggers) already in use.

2.1.2. Power Conversion Board

The power conversion board receives the battery power input, or the auxiliary power input, and converts it to levels for use in the supporting circuits of the Snow Probe. The microcontroller and interface circuitry use 5V at low current, while the sensor driver circuits use 5V and -5V, as well as 12V and -12V, both at moderate current levels. The spotlights (optional) run on 5V at high current levels.

2.1.3. The User Interface Board

The user interface board holds the three colored push buttons, the 7-segment LED display, the status indicator LEDs, and the spotlights. It accepts user input via the push buttons, and gives user feedback through the LEDs. For clarification of the letters used to spell words on the LED display . The individual components of the user interface board are described in detail below (see Section 2.2.).

2.1.4. Sensor Driver Board

The sensor driver board includes the circuitry that synthesizes and drives a fixed frequency, fixed amplitude sine wave across the sensor. The amplitude modulation of this signal is interpreted as change in permittivity size by the microcontroller. The board also contains the sampling circuitry which is conveyed to the microcontroller. Finally, the sensor driver board holds the proprietary pre-amplifier that directly connects to the sensor.

2.2. User Interface Components

The user interface components are those that provide feedback to you, as well as those that allow you to interact with the Snow Probe mesurement program. These include LEDs, speakers, and push buttons.

2.2.1. Push Buttons

Three buttons are used to control the actions of the Snow Probe program, including marking modifications to the existing program. In general, the center button is the "action" button. It is the one that initiates an action that the display indicates the unit is prepared for. For example, if the display indicates PASS, pressing the center button will proceed to allow you to enter a password. Pressing either of the arrow buttons will skip over an option or go back to the previous option (when possible). Note that PASS is not one of the options you can skip over! The keys are arranged as shown in Fig. 2.3.

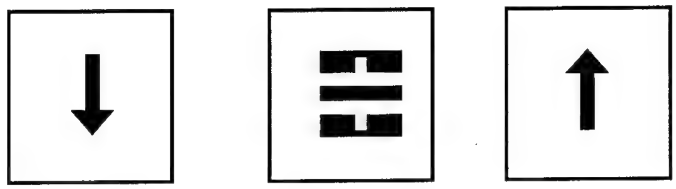

Decrease value Go to next menu or option	Choose menu or option	Increase value Go to previous menu or option

Figure 2.3. Push buttons configuration.

The green button ↓, on the left, is typically used to proceed <u>down</u> through the menus, to <u>decrease</u> a unit displayed on the LEDs, or to toggle between various setting options. It is also used in reviewing the permittivity/phase reading results.

The yellow button ↑, on the right, is typically used to proceed <u>up</u> through the menus, to <u>increase</u> a unit displayed on the LEDs, or to toggle between various setting options. It is also used to exit or escape from a mode or menu.

The red button ≡, in the center, is the Capacitec, Inc. trademark symbol. It is typically used to select a menu item to change or review, and then to verify the change as set with the arrow buttons. This is also the button used to begin and end gap readings.

For example, if you are setting the read time, the display shows RTIM. Pressing the ≡ button shows the current value, for example "4," pressing the up arrow will change the display to "5," while the down arrow changes it to "3." Pressing the ≡ button accepts the change and returns you to the RTIM screen.

During normal operation, depressing the center button will take the reading, while the ↓ button will skip back to the previous reading, and the ↑ button will skip over this reading to go to the next one.

2.2.2. LED Display

The 7-segment red LEDs provide a text interface display. This includes displaying menu items, current values, and the results of readings. The brightness can be adjusted for your convenience (see Section 3.4.3.). Lower intensity settings provide slightly longer battery life. The orientation of the display can be reversed in case the normal use is inverted.

2.2.3. Status Lights

There are three status lights above the LED display that provide additional feedback. Although their purpose varies with the different operations, the main menus are

identified with all of the status lights lit, and sub menu have only the two outside lights lit. If the screen is displaying a item that has a status of ON or OFF, the center light reflects the current value.

2.3.Snow Probe Kit Components

Each Snow Probe is shipped in a kit format and includes all of the components required to function in most measurement applications.

2.3.1. Case

The Snow Probe electronics and accessories are shipped in a watertight, shock-resistant Pelican™ case. An air-purge valve under the handle makes the unit airtight, and possibly difficult to open. If you have difficulty opening the case, make sure this valve is open.

Note:	The easiest way to open the case is one latch at a time, with one hand pressing down on the case, the other releasing the latch.

2.3.2. Snow Probe and Lance

A 2 meter extended snow "lance" is provided with a custom four screw connection to the snow probe. A coaxial extension cable and ground cord attachment extends from the end of this lance.

Rulered markings every 5mm are available to note depth.

2.3.3. Data/Power Connections and Cables

Three connectors on the rear of the unit provide auxiliary power to the Snow Probe electronics, RS232 interface to a personal computer, and analog voltage outputs. (optional)

2.3.3.1. Auxiliary Power

Although designed to run from four AA batteries, the electronics can also run from an external DC power supply or optional long life battery pack. The inputs must be 4.5V to 6V, capable of driving 600mA. The inputs are shown in Fig. 2.4.

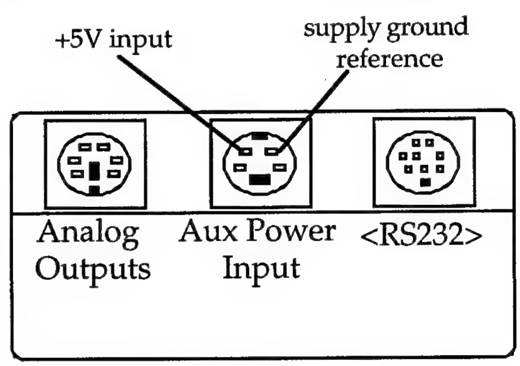

Figure 2.4. Auxiliary power connector.

2.3.3.2. RS232

The 8-pin RS232 interface connector allows the Snow Probe electronics to transmit data, reports, and user feedback to any terminal program running on any PC or Macintosh. It also allows you to control the program from the computer keyboard. This can be very useful during training, since the computer screen provides more feedback than the 7-segment display.

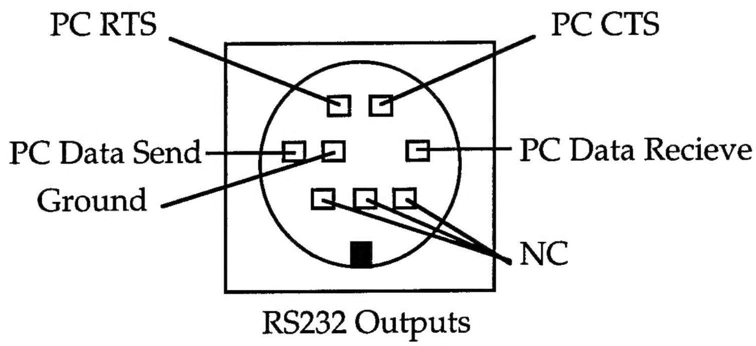

Figure 2.5. RS232 connector.

Any terminal program can be used, with communications set to 9600 baud, 8 bit, 1 stop bit and no parity checking (see your terminal software manual for further instructions regarding settings). A free terminal program, *monitor.exe*, is shipped with each unit. It can be used on any IBM compatible PC that can run DOS programs, and has been tested under Windows95 DOS emulation. For use with Macintosh computers, any terminal program will suffice, with communications settings as above.

2.3.3.3. Analog Output

The 6-pin analog output connector allows the electronics to set traditional analog voltage levels between 0V and 2.5V, dependent upon the display. The typical use of the analog output is as an "echo" of the value on the display, with some scaling factor. For example, a range of 0 to 4096 can be made to correspond to analog voltage levels between 0V and 1V. This voltage output could then be used by traditional data acquisition hardware that requires an analog voltage input (see Section 3.4.4. for details on turning the DACS on).

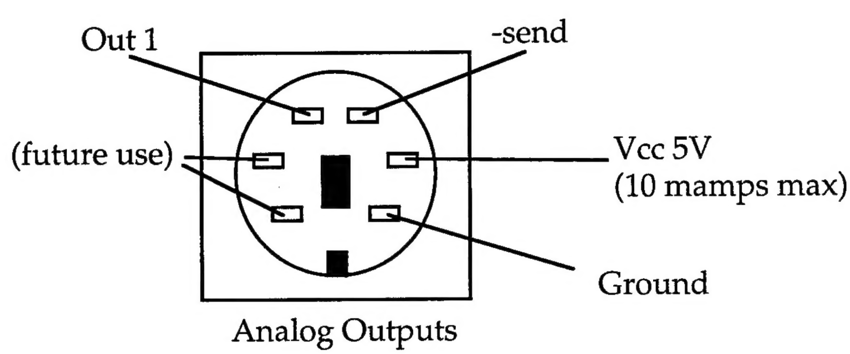

Figure 2.6. Analog output connector.

2.3.4. Ground Cable

The ground cable consists of a flexible, coiled, single conductor cable, with mating connectors at both ends. One connector snaps onto the side of the electronic enclosure.

The other end of the ground cable has an alligator clip. This end of the ground cable should be attached to the lance ground connection at the top of the snow probe.

Important!	The Snow Probe will not make accurate measurements without a proper ground connected to the Snow Probe or Snow Press.

2.3.5. Batteries

Two sets of four AA externally <u>rechargeable</u> alkaline batteries are supplied with each Snow Probe electronics. Each battery has a nominal output of 1.5V each, but the level drops as the battery is used. These batteries can be recharged up to 25 times without significant capacity loss. The manufacturer recommends that maximum number of recharge cycles can be attained by completely discharging the batteries before recharging. That is, wait until the Snow Probe electronics informs you that you need to change the batteries before doing it, if possible. Rechargeable alkaline batteries were chosen because they had the two features most desirable for the Snow Probe - reusability and high capacity. In addition, rechargeable alkalines are more environmentally friendly than most other rechargeable technologies. (Vendors for rechargeable alkalines are Rayovac and Pure Energy.)

The Snow Probe electronics can run on any 1.2V to 1.5V AA size battery. This includes standard and rechargeable alkalines, nickel cadmium (NiCad), or any other with this voltage rating.

Important!	The electronics cannot be used with 3.3V Lithium batteries. Do not use these batteries in the unit.

2.3.6. Battery Charger

An AC powered battery charger is included for recharging the rechargeable alkaline batteries. This charger should not be used with NiCad or any other rechargeable batteries, nor should it be used with non-rechargeable batteries. A typical time for recharging is about 4 hours. In addition to recharging, there is a receptacle area in the back of the charger for storing spare batteries. Note that they will not recharge when placed there.

For optimal battery life, the batteries should be discharged as far as possible before recharging. The batteries are ready to use when the charger's green LED turns on, but battery life can be extended by charging for longer periods of time. While a four hour charge is sufficient to use the batteries, an eight hour charge should be performed when possible.

3. GENERAL OPERATIONS

Connecting the Snow Probe to the electronics is accomplished with a single 3mm coaxial cable and ground lead. The ground lead is used to create a solid electronic reference. Choose a suitable "snow pit" area, and remove recent light snowfall, which may be cleared from the top of the snow pack. Otherwise, lance the snowpack until the extended 2m lance has penetrated by about 200mm. There are markings on the vertical "lance", which are graduated in 0.250" (6.35mm) steps. (others available) The current

portable electronics will prompt the operator with GP (general permittivity). Depress the center button, and a continuous reading begins. Move to a desired depth by tapping the top of the lance with a small mallet, or, if the snow pack is soft enough, push to the desired depth. Again, depress the center button to capture the local reading, and log the data. Repeat at each 0.25" (6.35mm) for a fine close group of measurement data. Generally, the tapping method yields better results because of the ice layers at various depths, which are difficult to "lance". (In the test, when pushing the snow probe down, an ice layer would resist, then suddenly break through - thereby missing several points due to overshooting.)

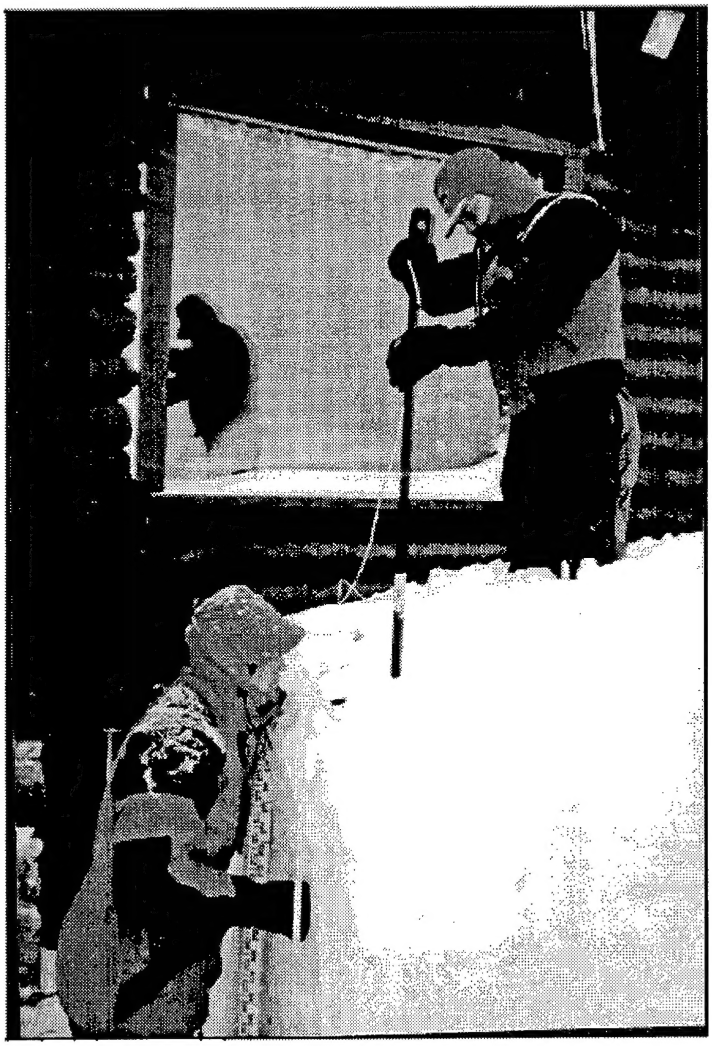

Snow Probe/Lance at Academic Snow Pit

3.1.1 Recording Readings

The portable electronics also have the ability to datalog the permittivity and phase delay at each reading point. In the data described in this paper, this feature was not ready at test time. Therefore, the data was recorded from separate analog outputs on the portable electronics to a portable dual trace oscilloscope.

Permittivity may be cross-correlated to density, and phaseshift to water content by comparing calibrated results from a detailed "academic snow pit" at the same site. Previous discussion of using a "Louge Snow Press" to calibrate the site is a most important tool in this effort.

3.1.2 Output Data

Once all the data points have been collected to a depth of 2.5 - 3 meters, there is an RS232 serial interface to download data to a P.C. The data is space delimited ASCII text, so that is can be nicely input to popular spread sheet programs.